

Enhancing reflection SNRs on seismic field data acquired using multiple vibrators driven by m-sequence pilots

Joe Wong and David Langton

ABSTRACT

In field tests using filtered m-sequence as quasi-orthogonal pilots to drive two or four vibrator sources simultaneously, we have found that reflections on the deblended common-source gathers are somewhat degraded by vibrator-to-vibrator crosstalk and by weak artifacts with moveouts running parallel to direct arrivals. Deeper analysis of the results lead us to conclude that crosstalk can be minimized by keeping the distance between adjacent vibrators to 100m or less. Also, judicious application of localized slant stacking to the deblended common-source gathers reduces the artifact amplitudes and increases the signal-to-noise ratios of reflections. We conclude that, by following these operational and processing steps, it is possible to efficiently conduct high-resolution 3D surveys with four vibrators controlled by m-sequence pilots and running simultaneously.

INTRODUCTION

Field-test have shown that it is possible to conduct seismic surveys using two or four vibrators driven by a set of filtered m-sequence pilot signals and running simultaneously (Wong and Langton, 2014; 2015a,b), Deblending of summed raw data recorded with simultaneous vibrators into separate common-source gathers (CSGs) occurs at the crosscorrelation step because the filtered m-sequences are quasi-orthogonal. In the context of Vibroseis acquisition, a quasi-orthogonal set has the following properties:

- (1) Within a restricted window of time lags, the autocorrelation of any member in the set closely approximates the delta function;
- (2) Within the same time window, the crosscorrelation between any two different members in the set is very nearly zero.

Deblending of summed multi-vibrator data driven by quasi-orthogonal pilots does not depend on differential time moveouts. Other Vibroseis pilot signals that have been tested for crosscorrelation orthogonality in simultaneous-source acquisition are variphase sweeps (Krohn et al., 2010), modified Gold codes (Sallas et al., 2011), and Galois codes (Thomas et al., 2010; 2012). Pecholcs et al. (2010) described a test 3D survey using 24 simultaneous vibrators controlled by variphase sweeps and modified Gold codes. Dean (2014) reviewed a variety of pseudorandom signals and their suitability as pilots for simultaneous multi-sourcing.

Our field tests have indicated that the artifacts resembling weak multiples of the direct arrivals and crosstalk noise exist on the deblended common-source gathers and interfere with reflection events. Both exist because the m-sequence pilots are not perfectly orthogonal. The crosstalk originates from large-amplitude ground roll and direct arrivals produced by adjacent and nearby vibrators. We will show that, for a four-vibrator source array, crosstalk interference can be kept to acceptable levels by limiting the source

spacing to 100m or less. Furthermore, we will show that local slant stacking reduces the amplitudes of both artifacts and crosstalk and so increases the signal-to-noise ratios (SNRs) of weak reflections. Local slant stacking as used in this article is equivalent to three-trace averaging along a range of slopes. The details are described in Appendix A.

SIMULTANEOUS SOURCE ACQUISITION WITH FOUR VIBRATORS

Figure 1 is a schematic representation of the acquisition geometry for field-testing four vibrators V1, V2, V3, and V4 running simultaneously with m-sequence pilots. We will present results for two cases in which the spacing between adjacent vibrators are set to 100m and 50m.

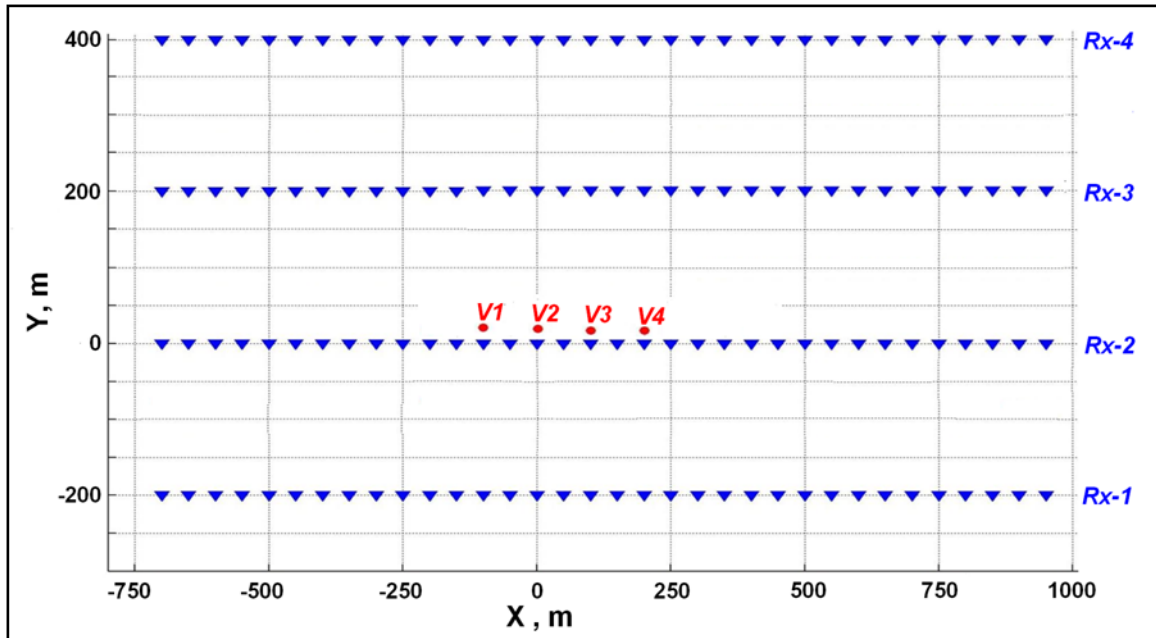


FIG. 1: Field configuration for testing four vibrators V1, V2, V3, and V4, separated by 100m and driven simultaneously by four quasi-orthogonal m-sequence pilots. The four receiver lines Rx-1 to Rx-4 are about 5800m long; the receiver interval is 50m. The distance between the line of vibrators and receiver line Rx-2 is about 5m.

The sweep times of the m-sequence pilots used in the field tests were designed to be 16.382 seconds. Acquisition was done with listen times (lengths of recorded raw data traces) of 22.000 seconds and a digital sampling interval of 2ms. Crosscorrelation of the blended raw field data with the appropriate m-sequence pilots yielded common-source gathers for the four vibrators.

As explained in the introduction, reflections on the extracted CSGs are somewhat contaminated by artifacts that have time moveouts data running parallel to the direct arrivals. The events from deeper reflectors at large source-receiver offsets are also partially obscured by crosstalk and random noise. In the following examples, we will show the extracted CSGs for the near-offset receiver line Rx-2 before and after artifact reduction and enhancement of reflection amplitudes.

Case 1: Vibrators separated by 100m

Figure 2 is the trace-normalized plots of blended uncorrelated data recorded for receiver line Rx-2 with a vibrator spacing of 100m. Note the strong low-frequency ground-roll noise for receivers inside the “noise cone”, i.e., at positions closest to the vibrators. The lateral extent of the noise cone is about 1200m. The low-frequency ground-roll is reduced before or after deblending by applying an Ormsby bandpass filter with corners at [15-30-100-150] Hz.

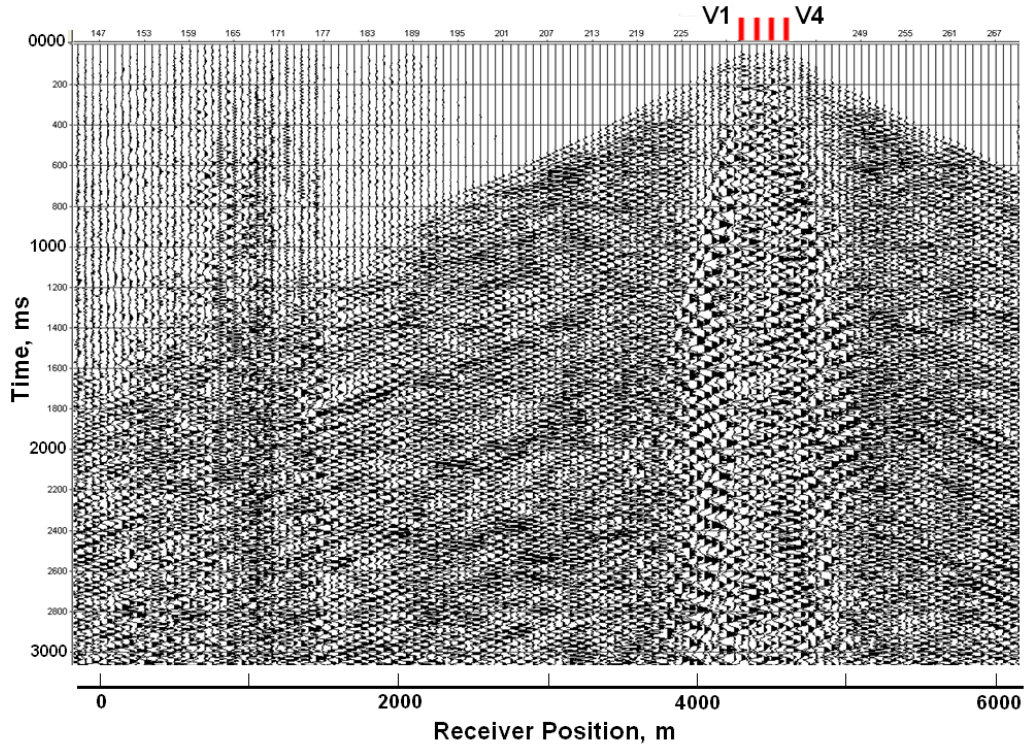


FIG. 2: Trace-normalized plot of the first 3000ms of unblended field data for receiver line Rx-2, recorded with four vibrators (source interval = 100m). Red lines show the positions of the four vibrators V1, V2, V3, and V4.

Filtered CSGs before artifact reduction and signal enhancement by local slant stacking are shown on the left side of Figure 3. We can see four reflections, but they are degraded by the first-arrival-related artifacts, and the amplitudes are fairly low relative to the crosstalk and random noise. The CSGs after artifact reduction and local slant stacking for signal enhancement are shown on the right side of the figure. The artifacts are reduced and the reflections stand out much more clearly above the background noise. The loss of reflection signal inside the noise cone remains an issue.

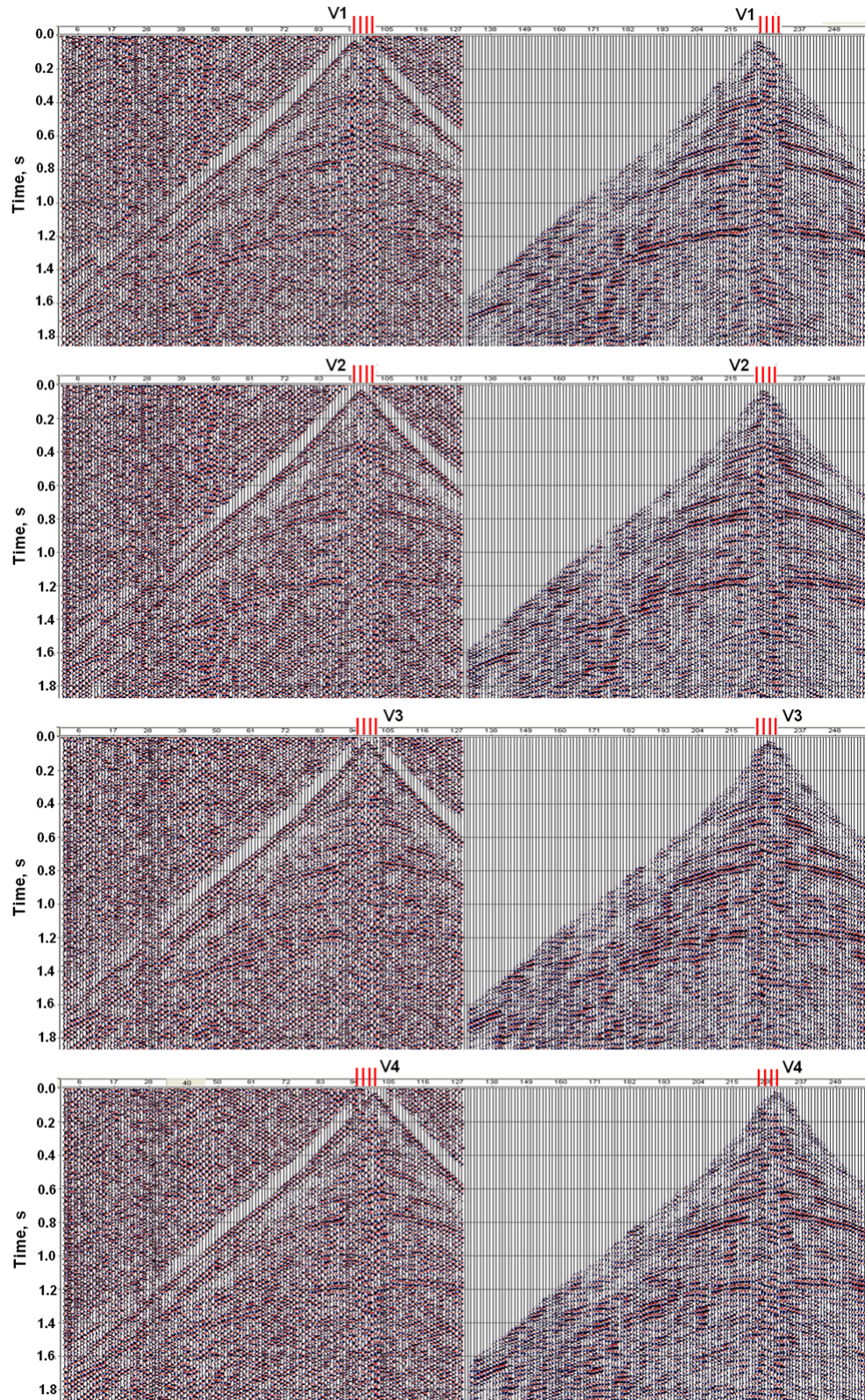


FIG. 3: AGC plots of extracted CSGs for vibrators V1, V2, V3, and V4 (source interval = 100m). Left: Bandpass filtering only. Right: After artifact reduction and signal enhancement.

Case 2: Four vibrators separated by 50m

Figure 4 is the trace-normalized plots of blended uncorrelated data recorded for receiver line Rx-2 with a vibrator spacing of 50m. Compared to the case where the vibrator spacing is 100m, the lateral extent of the ground roll “noise cone” has been reduced by half to about 600m. Again, the low-frequency ground-roll can be reduced by bandpass filtering, either before or after CSG extraction by crosscorrelation

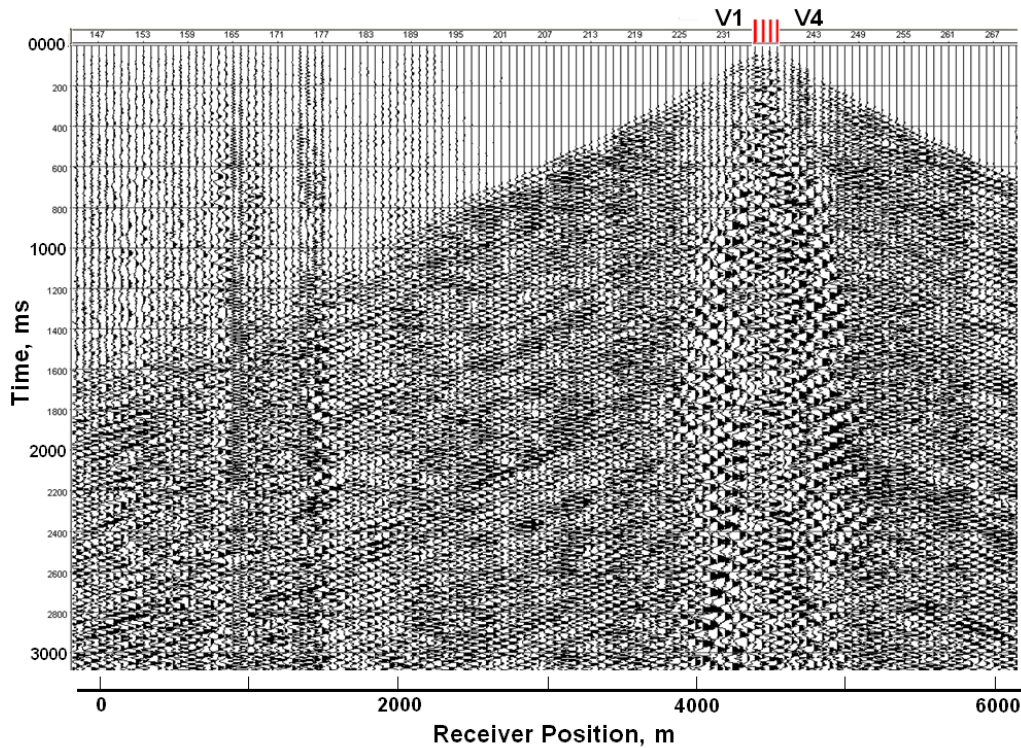


FIG. 4: Trace-normalized plot of the first 3000ms of unblended field data for receiver line Rx-2, recorded with four vibrators (source interval = 50m). Red lines show the positions of the four vibrators V1, V2, V3, and V4.

CSGs before artifact reduction and signal enhancement by local slant stacking are shown on the left side of Figure 5. As for the 100m-source-spacing case, we can see four reflections, but they are degraded by the first-arrival-related artifacts, and the amplitudes are fairly low relative to the crosstalk and random noise. The CSGs after artifact reduction and local slant stacking for signal enhancement are shown on the right side of the figure. The artifacts are reduced and the reflections stand out much more clearly above the background noise. The loss of reflection signal inside the noise cone is still an issue, but compared to 100m-source spacing case, less reflection signal is lost because lateral extent of the noise cone is less.

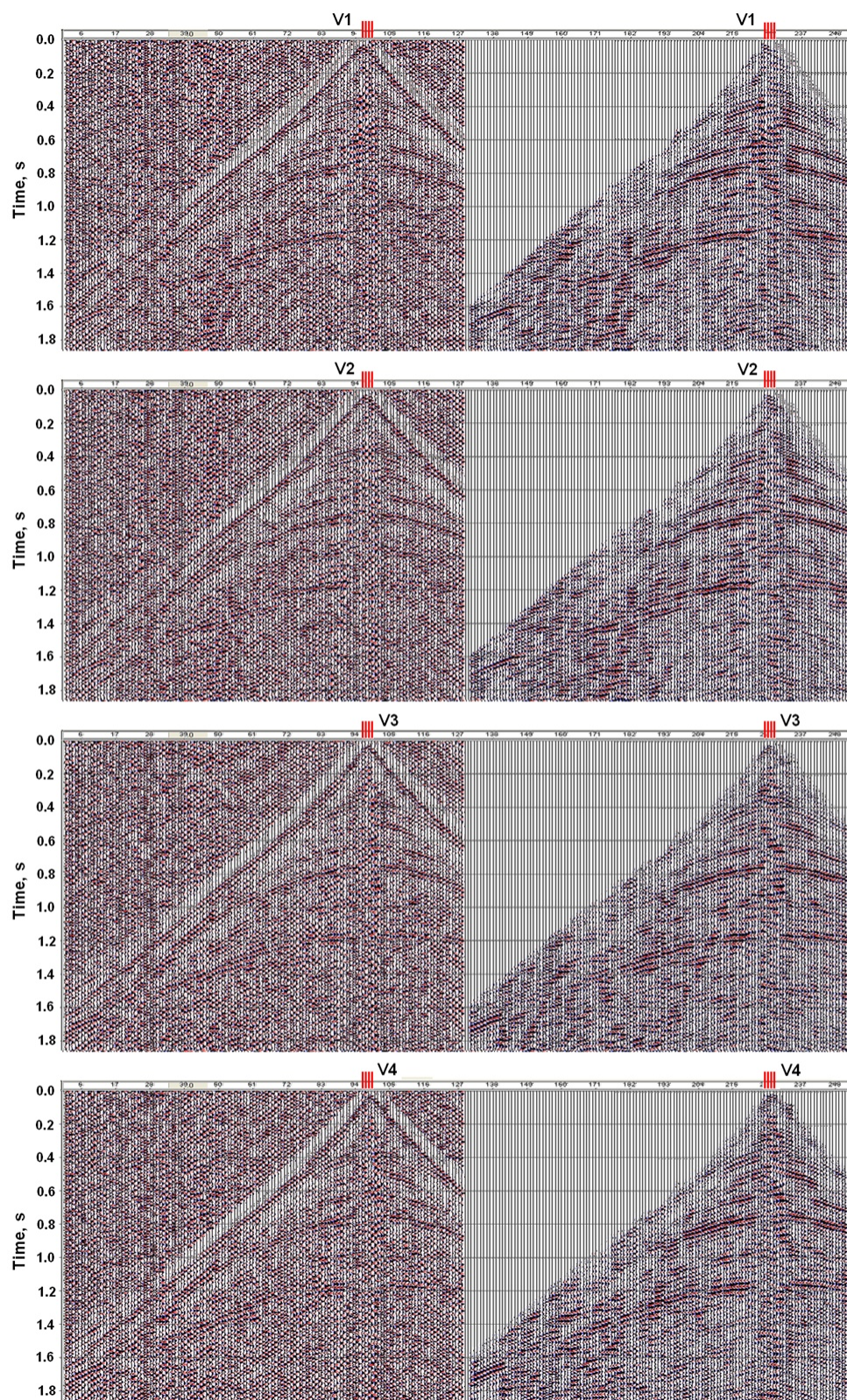


FIG. 5: AGC plots of extracted CSGs for vibrators V1, V2, V3, and V4 (source interval = 50m). Left: Bandpass filtering only. Right: After artifact reduction and signal enhancement.

CONCLUSIONS

We have assessed the quality of reflections on CSGs extracted from field data recorded with four vibrators running simultaneously with m-sequence pilots. Two cases were studied, in which the separation between adjacent vibrators were 100m and 50m. In both cases, common-source gathers obtained from the blended field data by crosscorrelation with the quasi-orthogonal m-sequence pilots show weak artifacts and crosstalk that degrade the quality of reflections.

The artifacts have the appearance of weak multiples of the first arrivals, i.e., they have time moveouts that run parallel to the first arrivals. We have devised an artifact cancellation procedure to reduce interference by the first-arrival-related artifacts. Crosstalk noise exists because the m-sequence pilots are not perfectly orthogonal. The most serious crosstalk interference is associated with the high-amplitude surface waves and first arrivals coming from nearby and adjacent vibrators, and is strongest for receivers located close to the vibrator sources, i.e., inside the ground-roll “noise cone”. Limiting the spacing between adjacent vibrators to 100m or less minimizes the spatial extent of the noise cone. We also have described a localized slant stacking step for enhancing weak reflections degraded by vibrator-to-vibrator crosstalk and random noise

On the basis of the above results, we draw the following conclusions:

1. Hydraulically-powered land vibrators can be controlled successfully by filtered m-sequences.
2. Quasi-orthogonal filtered m-sequences are effective pilots for practical simultaneous source acquisition with four vibrators if the spacing between adjacent vibrators is limited to 100m or less.
3. The deblending capability of quasi-orthogonal filtered m-sequences pilots used in simultaneous multi-source acquisition is improved if the pass band of the filtered m-sequences is adjusted to match the pass band of the earth reflection response.
4. A properly designed artifact cancellation processing step reduces the effects of first-arrival-related artifacts. Localized slant stacking is effective in increasing reflection amplitudes. Both procedures contribute to enhancing the SNRs of weak reflections obscured by crosstalk and other noise (see Appendix A for details).
5. For increasing the SNRs of very weak reflections on the deblended CSGs, other more sophisticated processing (involving all or some of the following procedures: ground roll removal, NMO and DMO alignment, trim statics, noise-signal separation, interpolation, FX deconvolution, and stacking) may be more effective than the steps outlined in the Appendix.

ACKNOWLEDGEMENTS

We thank Devon Energy Corporation for permission to present these results. Keith Radcliffe and Tom Phillips assisted in setting up the filtered m-sequence pilots for the vibrator controllers. CREWES is supported financially by its industrial sponsors, and also

is funded the Natural Sciences and Engineering Research Council of Canada (NSERC) through Grant CRDPJ-461179-13.

REFERENCES

- Dean, T., 2014, The use of pseudorandom sweeps for vibroseis surveys: *Geophysical Prospecting*, **62**, 50-74.
- Krohn, C., Johnson, M., Ho, R., and Norris, M., 2010, Vibroseis productivity: shake and go, *Geophysical. Prospecting*, **58**, 102-122.
- Pecholcs, P., Lafon, S. K., Al-Ghamdi, T., Al-Shammery, H., Kelamis, P. G., Huo, S. X., Winter, O., Kerboul, J.B., and Klein, T., 2010, Over 40,000 vibrator points per day with real-time quality control: opportunities and challenge: 80th International Annual Meeting, SEG, Expanded Abstracts, **29**, 111-115.
- Sallas, J., Gibson, J., Maxwell, P., and Lin, F., 2011, Pseudorandom sweeps for simultaneous sourcing acquisition and low-frequency generation: *The Leading Edge*, **30**, 1162-1172.
- Thomas, J.W., Jurick, D.M., and Osten, D., 2012, Vibroseis as an impulsive seismic source - 3D field testing Permian Basin Texas: 82nd International Annual Meeting, SEG, Expanded Abstracts, 86-90.
- Thomas, J.W., Chandler, B., and Osten, D., 2010, Galcode: simultaneous seismic sourcing: 80th International Annual Meeting, SEG, Expanded Abstracts, 86-90.
- Wong, J., and Langton, D., 2014, Field testing of multiple simultaneous vibrators controlled by m-sequences: 84th Annual International Meeting, SEG, Expanded Abstracts, 173-177.
- Wong, J., and Langton, D., 2015a, Wong, J., and Langton, D., 2015a, Simultaneous multi-source acquisition using m-sequences: CREWES Research Report, **27**, 73.1-73.21.
- Wong, J., and Langton, D., 2015b, Field and numerical investigation of filtered m-sequence pilots for Vibroseis acquisition: 85th Annual International Meeting, SEG, Expanded Abstracts, 196-200.

APPENDIX A

Local slant stacking

For each digital point on a given trace of an input CSG, we sum and average its value and two values from the immediately preceding and following traces. The immediately adjacent values are taken from points along a given slope, and the calculation is done over a range of slopes. The averaged sum over this range having the maximum absolute value is retained (together with its sign) and assigned to a new CSG.

Enhancing reflection SNRs

The following processing steps reduce ground roll noise, attenuate interference from artifacts that appear as first-arrival multiples, and increase the signal-to-noise ratios of reflection events.

1. Extract the CSG associated with each vibrator in the array by cross-correlation of the blended raw field with the appropriate m-sequence pilot. Figure A1(a) displays an example of an extracted CSG in an AGC plot using an AGC window length of 200ms.
2. Figure A1(b) is an AGC plot of the CSG after bandpass filtering to reduce ground-roll noise. On this figure, we see artifacts appearing as weak multiples of the first arrivals. These artifacts obscure the reflection events, especially those occurring at later times.
3. We now apply pre-processing to reduce interference caused by the first-arrival-related artifacts. First, we obtain accurate first-break times that accurately follow

the moveouts of the first arrivals. Then we shift the seismograms according to these first-break times to align all the first arrivals to zero time. The CSG of aligned seismograms is displayed on Figure A2(a).

4. We next produce an estimate of events on the shifted CSG with zero time moveout by doing a three-trace running average on the aligned gather, so that an estimated trace is the average of the trace and the two traces immediately before and after the trace. The gather of averaged traces is plotted on Figure A2(b). The short, flat-appearing events on this gather are the estimates of the artifacts.
5. The interference by artifacts is reduced by subtracting the averaged aligned data from the unaveraged aligned data. Figure A3(a) is the plot of this difference, and we can see that events with non-zero time moveout appears more clearly.
6. We reverse the trace alignments on the difference CSG and restore the hyperbolic shape of the original CSG. Finally, we apply local slant stacking to enhance the SNRs of reflections. The result is plotted on Figure A3(b).

Figure A4 is a direct comparison of the bandpass-filtered input CSG of Figure A1(b) and the final output CSG of Figure A3(b). The comparison shows that the reflection events appear with much improved clarity after the application of the above processing steps. This is especially true for the deepest event below about 1150ms. However, they have not improved the appearance of events inside the ground roll “noise cone” at receiver positions between 4600m and 5200m.

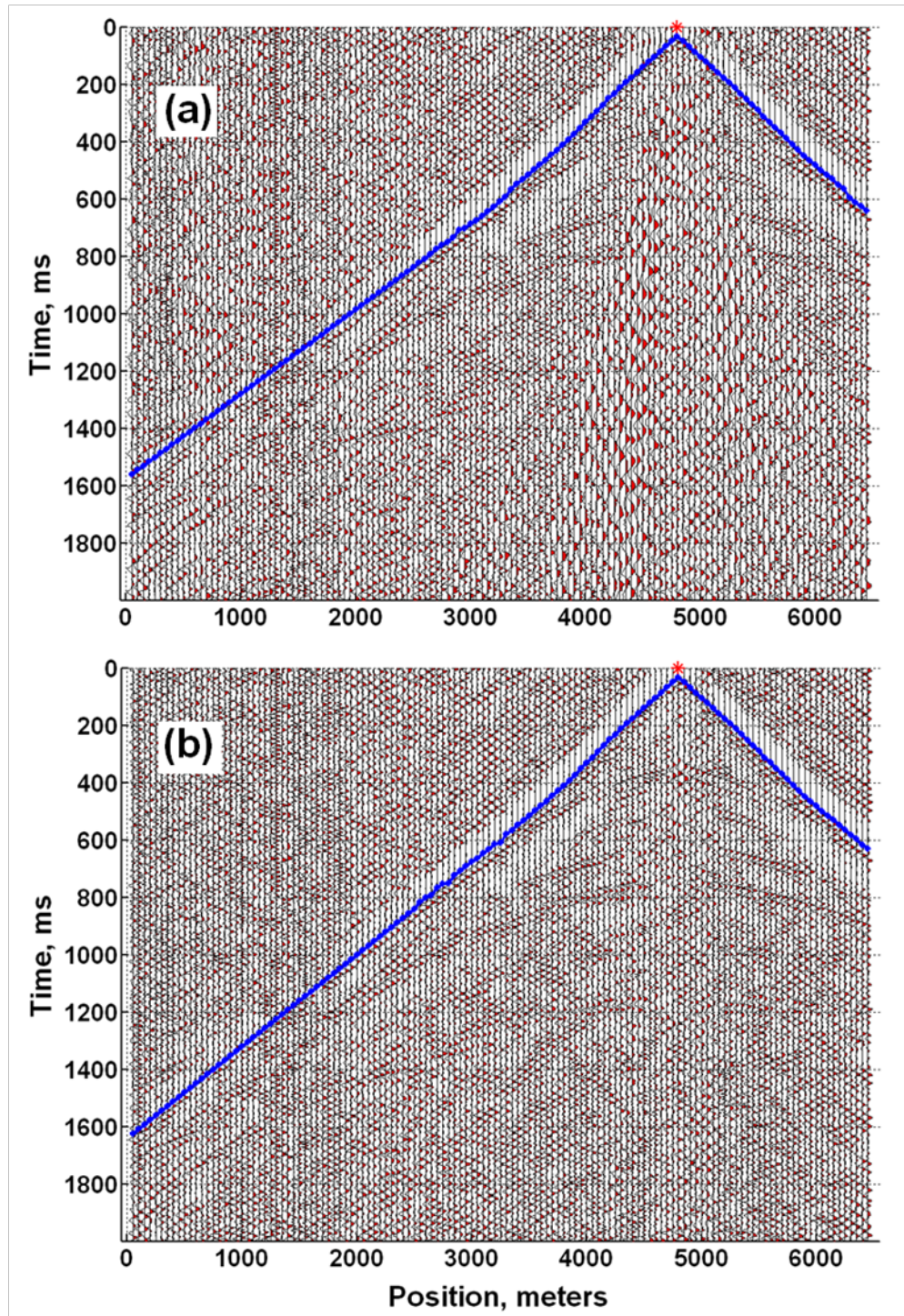


FIG. A1: A common-source gather extracted from blended field data recorded with four vibrators running simultaneously, (a) AGC plot before bandpass filtering, and (b) AGC plot after bandpass filtering. First arrival times are plotted as the blue lines.

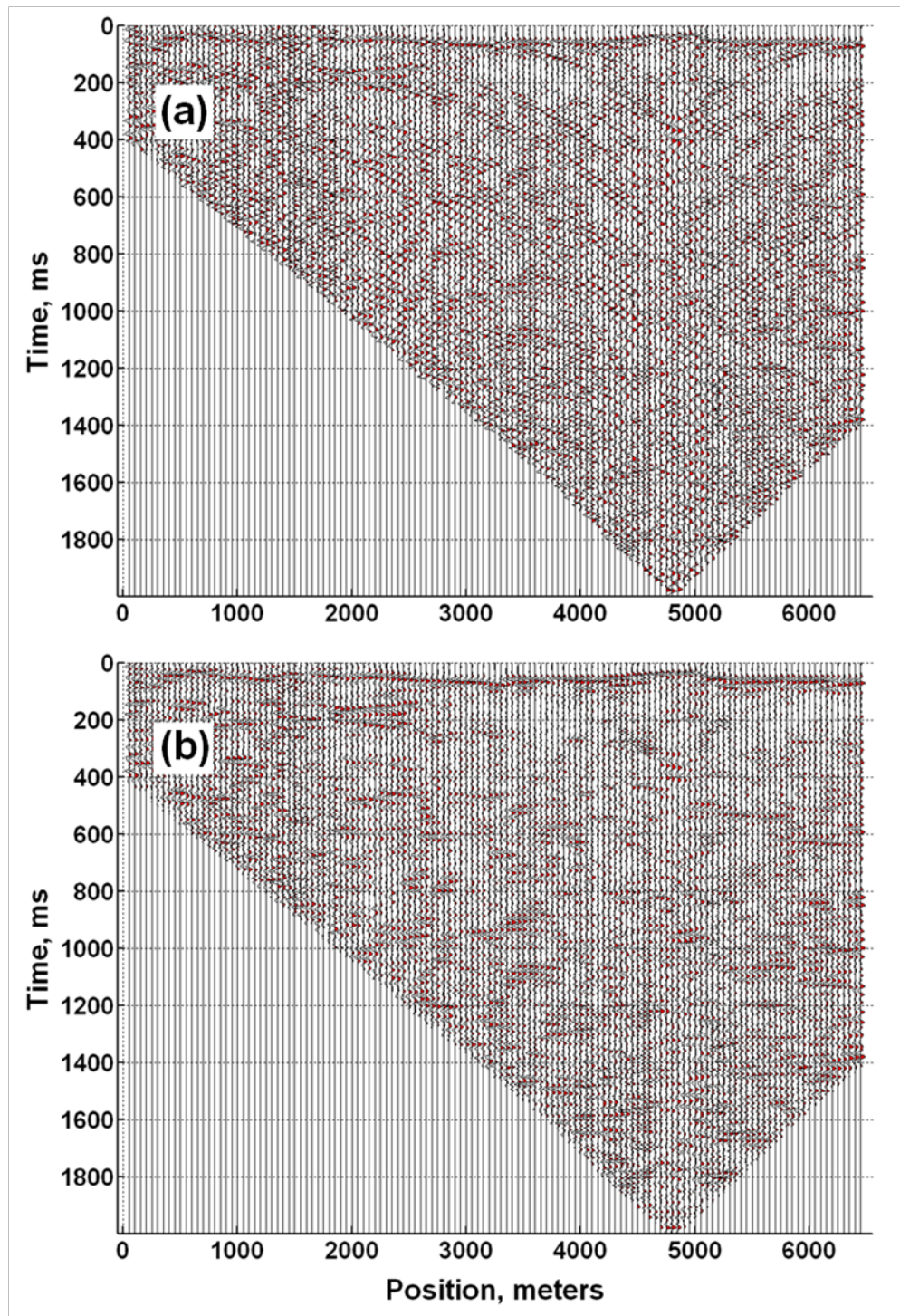


FIG. A2: (a) The data of Figure 1(b) CSG after trace alignment to the first-arrival times; (b) CSG generated from the aligned data by three-trace summing along lines of zero time moveout.

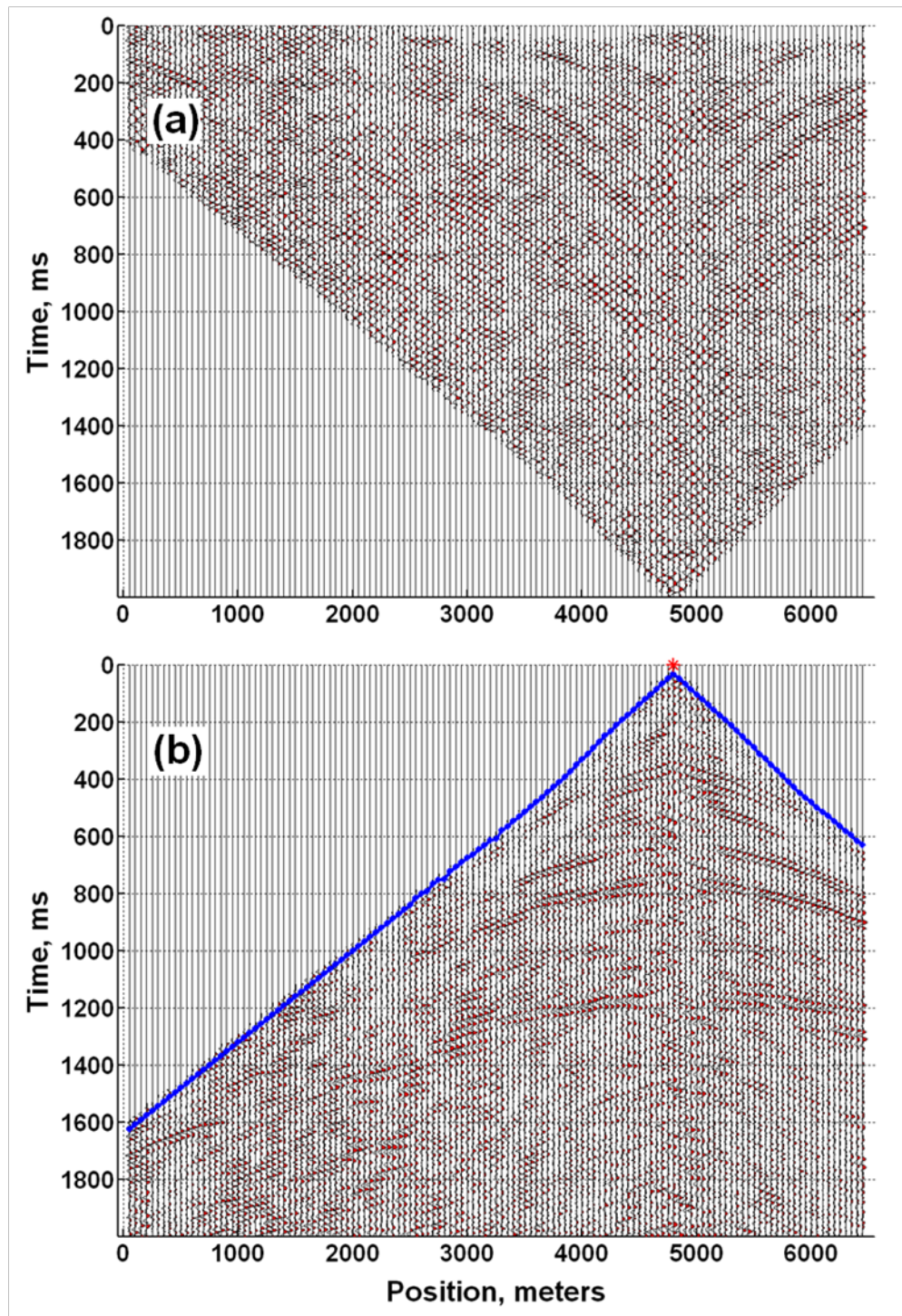


FIG. A3: (a) The result of subtracting the data of Figure A2(b) from the data of A2(a). (b) The CSG that results from reversing the alignment, and enhancing the reflection SNRs by a local slant stacking

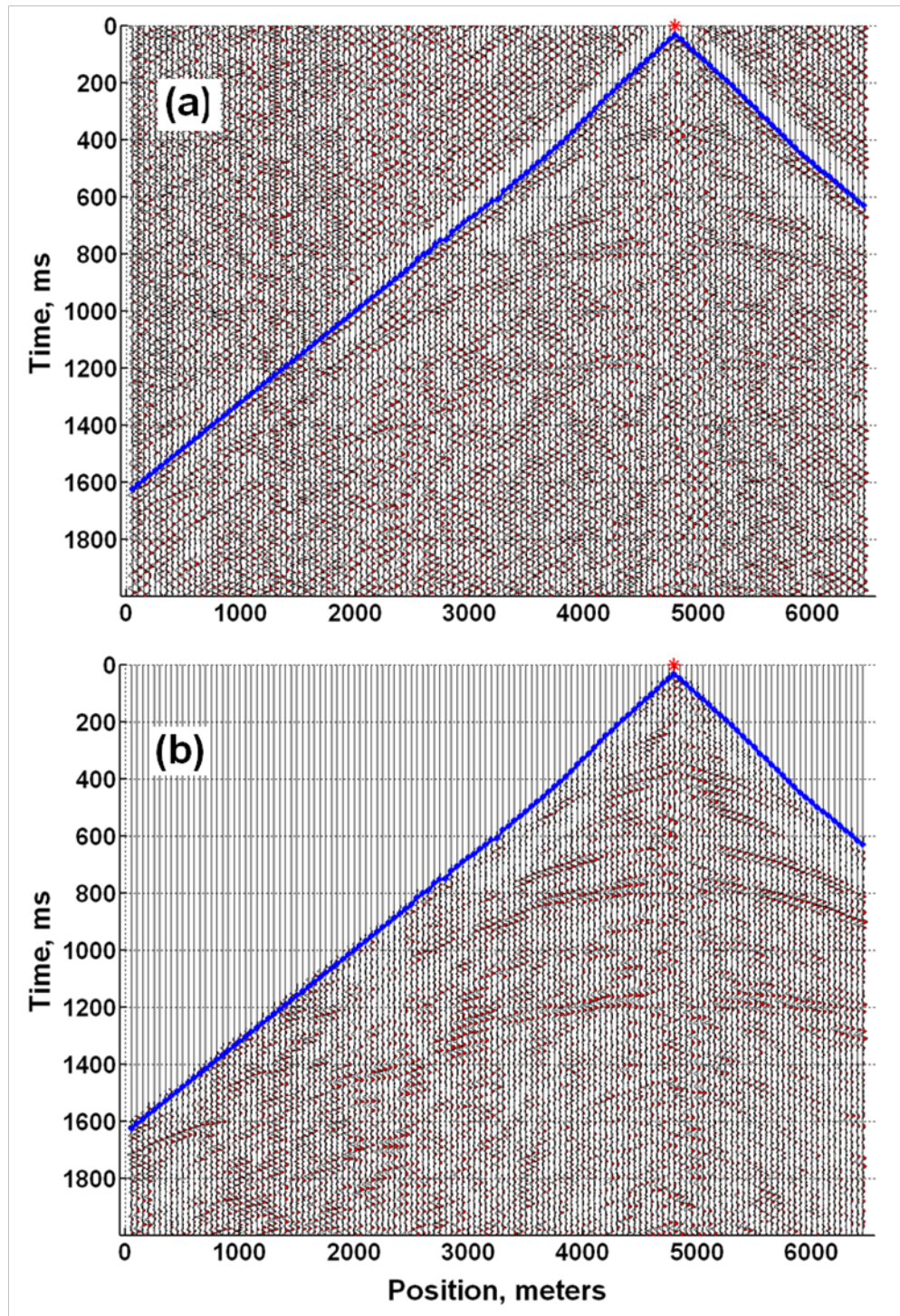


FIG. A4: Direct comparison of the bandpass-filtered input CSG of Figure A1(b) and the final output CSG of Figure A3(b).